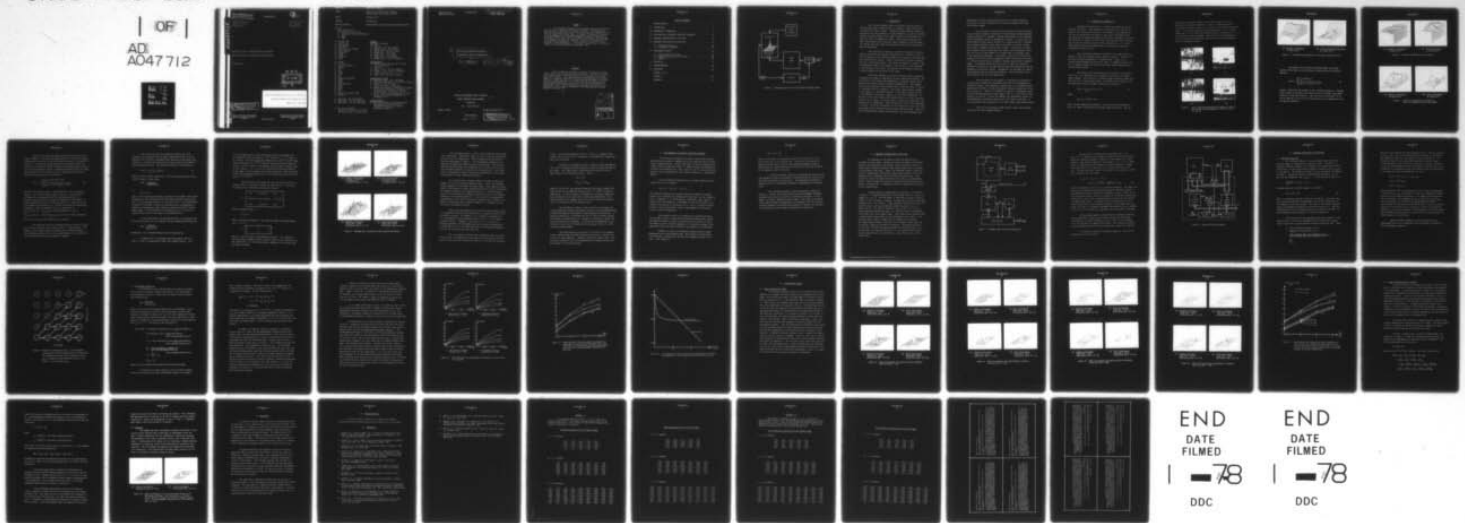AD-A047 712   DEFENCE RESEARCH ESTABLISHMENT VALCARTIER (QUEBEC)   F/G 17/8
DIGITAL AREA CORRELATION TRACKING BY SEQUENTIAL SIMILARITY DETE--ETC(U)
NOV 77   C MUNTEANU
UNCLASSIFIED   DREV-R-4097/77   NL

| OF |
ADI
A047712

END
DATE
FILMED
—78
DDC

END
DATE
FILMED
—78
DDC

UNCLASSIFIED

③
NV

CRDV RAPPORT 4097/77
DOSSIER: 3621J-003
NOVEMBRE 1977

DREV REPORT 4097/77
FILE: 3621J-003
NOVEMBER 1977

DIGITAL AREA CORRELATION TRACKING

BY SEQUENTIAL SIMILARITY DETECTION

C. Munteanu

D D C

RECEIVED

DEC 19 1977

B

Centre de Recherches pour la Défense

Defence Research Establishment

Valcartier, Québec

BUREAU - RECHERCHE ET DEVELOPPEMENT
MINISTÈRE DE LA DÉFENSE NATIONALE
CANADA

NON CLASSIFIÉ

RESEARCH AND DEVELOPMENT BRANCH
DEPARTMENT OF NATIONAL DEFENCE
CANADA

(6) DIGITAL AREA CORRELATION TRACKING

BY SEQUENTIAL SIMILARITY DETECTION,

by

(10) C. Munteanu

(11) Nov 77

(12) 51 p.

CENTRE DE RECHERCHES POUR LA DEFENSE

DEFENCE RESEARCH ESTABLISHMENT

VALCARTIER

Tel: (418) 844-4271

Québec, Canada

November/novembre 1977

NON CLASSIFIE

404 945

i

RESUME

La corrélation d'images est une méthode efficace de poursuivre
une cible qui ne possède pas de traits saillants. Ceci implique la
détection d'une cible dans son milieu au moyen des similitudes qu'elle a
avec une image étalon de la cible. Ce rapport présente une évaluation
de la performance de l'algorithme séquentiel pour la détection de la
similarité (ASDS) dans la détection numérique d'images. On montre que
la performance de l'ASDS est comparable à celle de la méthode courante
de corrélation mathématique. Les deux techniques sont décrites et
essayées sur des photographies. Une évaluation analytique de l'ASDS ap-
pliquée à des images binaires est présentée. (NC)

ABSTRACT

Area correlation tracking is an effective method of tracking
targets that do not have salient characteristics. This involves detect-
ing a target within a scene by means of its similarity with a stored
image of the target. This report presents an evaluation of the perfor-
mance of a sequential similarity detection algorithm (SSDA) in the task
of digital image detection. It is shown that the performance of the
SSDA is highly competitive with that of the widely used mathematical
correlation method. Both techniques are reviewed and tested on still
photographs. An analytical evaluation of the SSDA applied to binary
images is presented. (U)

TABLE OF CONTENTS

Figure 1 - Configuration for area correlation tracking system

1.0 INTRODUCTION

Most current imaging seekers are based on the detection of a predetermined target characteristic, or signature, within the scenery to identify and track a target. Contrast and edge-tracking seekers use occurrences of large gradients in image brightness as clues for tracking. Centroid tracking schemes utilize edge-tracking of the boundaries of a target to track its geometrical center. These simple techniques lose their effectiveness when a distinct target signature is not available, for instance when the target lacks prominent features and high contrast with the background.

Area correlation tracking is an effective method of tracking targets that do not have salient characteristics. Essentially this involves matching a stored reference image of the target to real-time scene data obtained from a sensor. Figure 1 illustrates a typical configuration of a correlation tracker. The correlator computes a surface or map of coefficients which are a measure of the similarity of the reference to all portions of the scene. The location of the maximum coefficient is used to update the aim point of the sensor.

This report examines two classes of digital image correlation techniques with regard to application to area correlation tracking. The first class is the widely used mathematical correlation method, which performs correlation exactly as defined mathematically. The simplest form of this technique is the matched filter, where the scene is directly correlated with the reference. This filter, whose impulse response is the signal it is intended to detect, is the optimal linear solution to the problem of detecting a signal in a white noise background. In the case of real-life scenery, the matched filter is, in fact, not appropriate, since a target in a natural scene is generally significantly correlated with its background. Hence the premise of white noise background is invalid. The filter performance can be optimized by using other reference images derived from the original target reference image. These references significantly reduce the correlation with the background while

maintaining relatively good correlation with the original reference. In Section 2.0, these techniques are reviewed and demonstrated using two different images.

For an automatic digital tracking system utilizing the mathematical correlation method, the necessity of generating an image-dependent optimum reference is a drawback. Another disadvantage of this technique is the considerable amount of computation involved. In particular, this method spends an equal amount of effort in determining that a reference and a candidate portion of the scene do not match as it does in determining that a reference-candidate pair matches. Intuitively, determining a mismatch should require much less effort than determining a match. This has led to the development of a second class of techniques, that of the sequential algorithms. In particular, Section 3.0 examines the sequential similarity detection algorithm (SSDA) of Barnea and Silverman [1], which was presented as a method of digital registration of multiple images. By spending relatively little time in regions of reference-candidate dissimilarity, the SSDA requires much less computation than the mathematical correlation method. Furthermore, the SSDA does not require image preprocessing for successful operation. These attributes make it very attractive for real-time application.

The main purpose of this paper is to present an evaluation of the SSDA and to compare its performance with that of the mathematical correlation method. The underlying interest here is in a hardware implementation of the SSDA, for which a proposed tracking configuration is given in Section 4.0. Section 5.0 presents an analytical performance evaluation of the SSDA applied to binary images, that is, images that are digitized to two levels. Section 6.0 compares the experimental results of the mathematical correlation (Section 2.0) with those of the SSDA. It also investigates the improvement of the SSDA through image preprocessing.

This work was performed at DREV between January and September 1976 under PCN 21J03 "Imaging Seekers".

2.0 MATHEMATICAL CORRELATION

Mathematical correlation is a widely used technique for the detection of images. Since mathematical correlation is a form of convolution, the correlation surface, or correlogram, can be obtained as the inverse transform of the product of the Fourier transform of the reference and the complex conjugate of the Fourier transform of the scene. This technique is popular in the digital domain because of the development of the fast Fourier transform (FFT) algorithm [2, 3, 4]. (It is also popular in the analog domain because of the Fourier transform properties of lenses [5, 6].)

The correlation techniques described in this report have been applied to two very different images, shown in Figure 2. Figure 2a is an aerial infrared photograph of a highway scene. Figure 2c is a visible light photograph of a military truck. In Figure 2b and 2d, the 16 x 16 element targets and the 48 x 48 element search scenes are outlined by white squares.

The simplest form of mathematical correlation is the matched filter [7, 8, 9], where the filter response is matched to the target signal (image). Let W be an M x M element target (reference) image, and let S be an L x L element scene image. The matched filter output is the two-dimensional cross-correlation surface $R(u,v)$ given by

$$R(u,v) = \sum_{ij} S_{uv}(i,j)\, W(i,j) \tag{1}$$

where

$$S_{uv}(i,j) = S(u+i,\ v+j).$$

$R(u,v)$ can be computed using the FFT. The location of the maximum of $R(u,v)$ is taken to be the point of maximum image similarity. This may

give incorrect results, however, since regions where S is large
may produce the maximum correlation. This is demonstrated in the
correlograms of Figure 3 where (1) is applied to the highway and truck
images. (In all the highway and truck correlograms, M = 16, u and v
range from -16 to +16, and the correlation peak is expected at u = v = 0
at the center of the correlogram. Moreover, all the correlograms of
this section record the absolute value of R(u,v) and are normalized
to have a maximum of unity.)
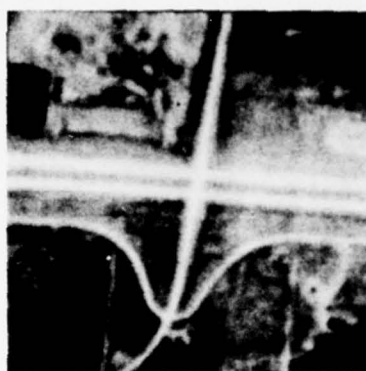
(a)   (b)
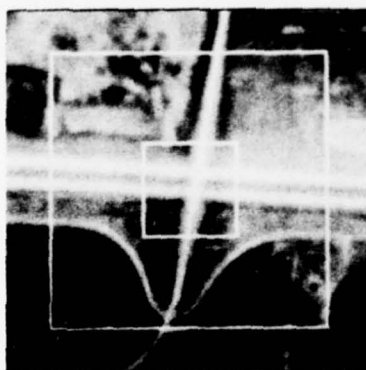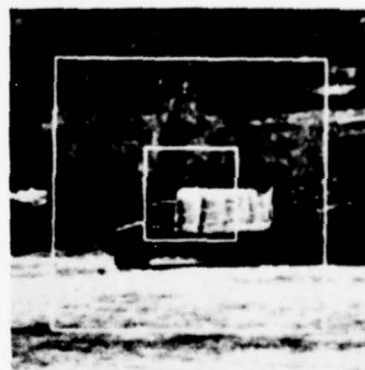
(c)   (d)

Figure 2 - Aerial infrared photograph of highway (a) and (b)
and visible light photograph of military truck
(c) and (d)
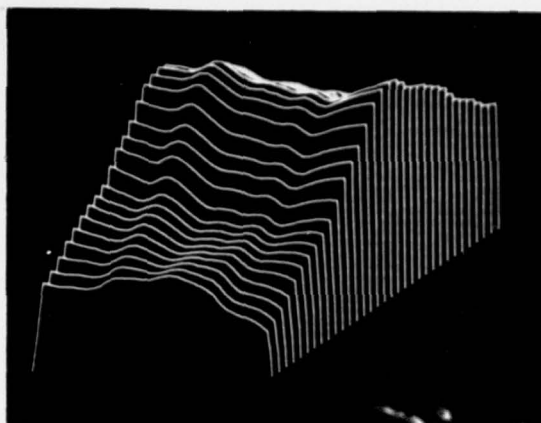
(a) Highway correlogram
     No image noise
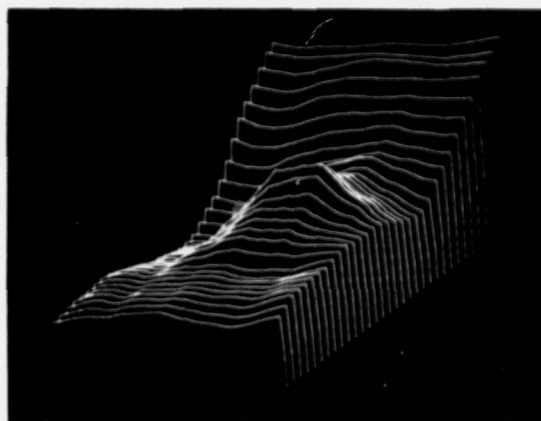
(b) Truck correlogram (rearview)
     No image noise

Figure 3 - Un-normalized mathematical correlation (matched filter)

The problem of the target correlating highly with bright regions of the scene can be rectified by normalizing the correlation function:

$$R(u,v) = \frac{\sum\limits_{ij} S_{uv}(i,j)W(i,j)}{[\sum\limits_{ij} S_{uv}^2(i,j)]^{\frac{1}{2}}[\sum\limits_{ij} W^2(i,j)]^{\frac{1}{2}}} \qquad (2)$$

Figure 4 illustrates the results of this correlation measure. Although correct peaks are provided, the surfaces tend to be broad, which makes detection of the peak difficult. Note that only the numerator of (2) can be computed with the FFT; the normalization of the denominator must be computed separately.
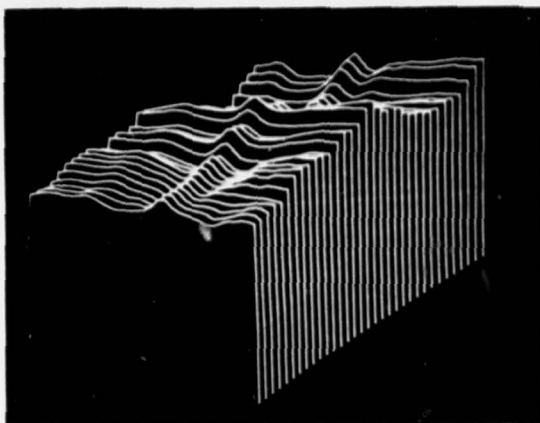
(a) Highway correlogram
No image noise
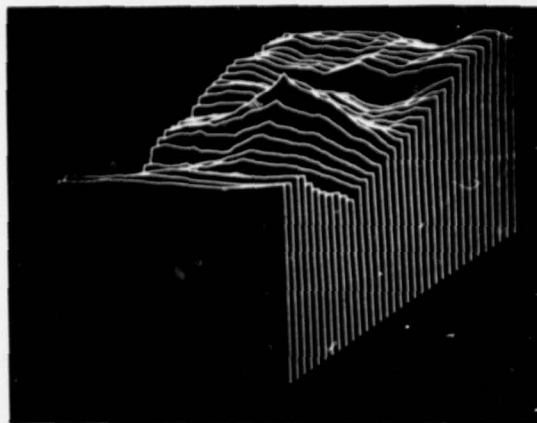
(b) Truck correlogram
No image noise

Figure 4 - Normalized mathematical correlation
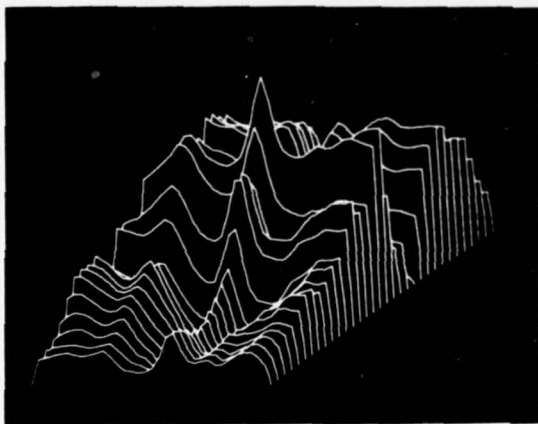
(a) Highway correlogram
No image noise
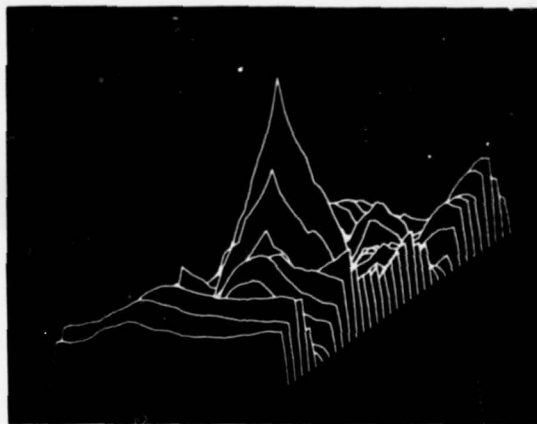
(b) Truck correlogram
No image noise

Figure 5 - Normalized mathematical correlation
(with dc component removed from images)

Thus far, the images have been represented as arrays of non-negative numbers. This gives the images positive dc levels that produce a large positive dc level in the correlation function (as is evident in Figure 4). A correlation dc level provides no information about the location of the peak but reduces the peak to background (signal-to-noise) ratio of the correlation surface. Improved peak detectability can therefore be expected if the target dc level is subtracted from both the target and the scene prior to correlation:

$$R(u,v) = \frac{\sum_{ij}\sum(S_{uv}(i,j)-\overline{W})\ (W(i,j)-\overline{W})}{[\sum_{ij}\sum(S_{uv}(i,j)-\overline{W})^2]^{\frac{1}{2}}[\sum_{ij}\sum(W(i,j)-\overline{W})^2]^{\frac{1}{2}}} \tag{3}$$

where $\overline{W}$ is the target dc level. The improvement of this is shown in Figure 5. It is worth noting, perhaps, that (3) is not equivalent to removing the dc component from the correlogram given by (2). Although this has been verified with the highway and truck images, a simple argument will serve to illustrate the point. Consider the case of un-normalized correlation, i.e. (2) and (3) without the normalizing denominator. Then the numerator of (3) is equivalent to
$\sum_{ij}\sum S_{uv}(i,j)W(i,j) - \overline{W} \sum_{ij}\sum S_{uv}(i,j)$ and the numerator of (2) is
$\sum_{ij}\sum S_{uv}(i,j)W(i,j)$. Since $-\overline{W} \sum_{ij}\sum S_{uv}(i,j)$ is not a dc term, the numerators of (2) and (3) do not differ by a dc component.

The difficulty with the correlation measures given by (1) and (2) is due to the nature of the signal, that is, natural imagery. The problem is that natural images are rather highly correlated signals. The correlation measure (3) is a very simple attempt to decorrelate the image by removing the dc (zero frequency) component.

The correlation peak can be sharpened further by a more elaborate processing that acts on higher frequencies as well as on dc. Reference [10] describes an optimum filter operating on the target that generates a reference that maximizes the signal-to-noise ratio (SNR) of the correlation function. The correlation surface is now defined as

$$R(u,v) = \sum_{ij}\sum S_{uv}(i,j)\hat{W}(i,j) \tag{4}$$

where $\hat{W}$ is the filtered version of W. The filter that maximizes the correlation signal to noise ratio

$$SNR = \frac{E[R(0,0)]}{(var[R(u,v)])^{\frac{1}{2}}}$$

is

$$\underline{\hat{W}} = \Sigma^{-1}\underline{W}$$

where E is the expectation operator, $\underline{W}$ and $\underline{\hat{W}}$ are row-scanned vector representations of the reference and of the filtered reference respectively, and Σ is the covariance matrix of $\underline{W}$. The action of Σ^{-1} is to decorrelate or whiten the reference so that its correlation with the background is reduced to a much greater extent than its correlation with the original target image. If the reference is uncorrelated, the Σ^{-1} will be the identity matrix and (4) will reduce to the matched filter.

In this application, the correlation matrix is used rather than the covariance matrix so as to maximize the more demanding SNR expression

$$SNR = \frac{E[R(0,0)]}{(E[R^2(u,v)])^{\frac{1}{2}}}$$

Henceforth, Σ will therefore denote the correlation matrix.

In applying (4) to the highway and truck images, the very large Σ^{-1} matrix is approximated rather than computed exactly. As in

[10], the submatrices of image row autocorrelation are assumed to be of exponential form such that the $(i,j)^{th}$ element is $\rho_1^{|i-j|}$, where ρ_1 is a scalar. The cross-correlation submatrices of the mth and n^{th} image rows are assumed to be $\rho_2^{|m-n|}$ times the row autocorrelation submatrix, where ρ_2 is also a scalar. (This departs slightly from the example given in [10], where $\rho_1 = \rho_2 = \rho$, so as to account for different properties of the image in the horizontal and vertical directions.) What this means is that the correlation between the $(i,j)^{th}$ element and the $(m,n)^{th}$ element is $\rho_1^{|i-m|}\rho_2^{|j-n|}$.

Multiplication of the image vector by the inverse of this correlation matrix is equivalent (except for edge effects) to convolving the image with the following point spread function:

$$
h = \begin{bmatrix}
\rho_1\rho_2 & -\rho_2(1+\rho_1^2) & \rho_1\rho_2 \\
-\rho_1(1+\rho_2^2) & (1+\rho_1^2)(1+\rho_2^2) & -\rho_1(1+\rho_2^2) \\
\rho_1\rho_2 & -\rho_2(1+\rho_1^2) & \rho_1\rho_2
\end{bmatrix}
$$

The new reference then is

$$\hat{W} = h * W$$

where * indicates convolution. Note that for highly correlated images, $(\rho_1 \to 1,\ \rho_2 \to 1)$,

$$
h = \begin{bmatrix}
1 & -2 & 1 \\
-2 & 4 & -2 \\
1 & -2 & 1
\end{bmatrix}
$$

which is a form of spatial differentiation operator. This emphasizes the high spatial frequency content (such as edges) of the reference, and thus effectively it is the high-frequency components of the images that are being correlated.
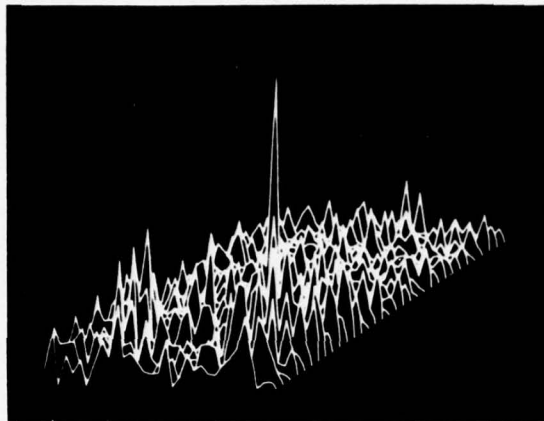
(a) Highway correlogram
No image noise
Correlation SNR = 17.3 db
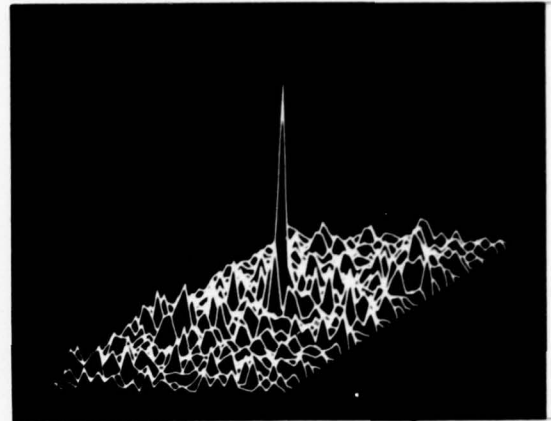
(b) Truck correlogram
No image noise
Correlation SNR = 23.3 db
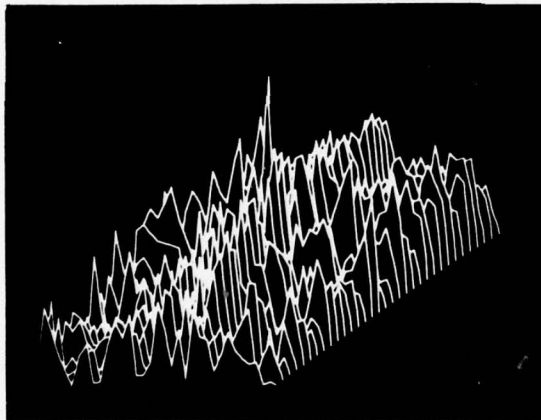
(c) Highway correlogram
Image SNR = 10 db
Correlation SNR = 11.1 db
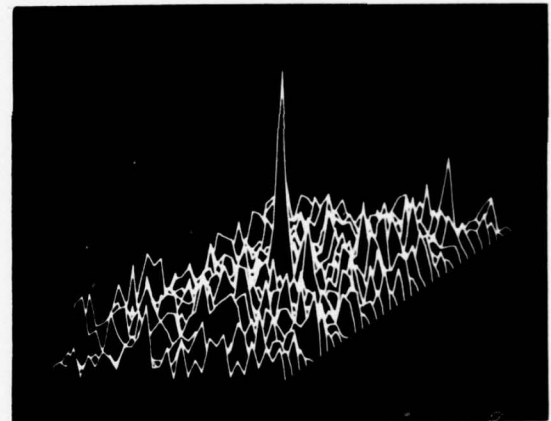
(d) Truck correlogram
Image SNR = 10 db
Correlation SNR = 18.6 db

Figure 6 – Mathematical correlation using whitened references

For the highway image, ρ_1 and ρ_2 were estimated to be 0.99 and 0.95 respectively. Appropriate values of ρ_1 and ρ_2 for the truck image were 0.97 and 0.93 respectively. These estimates were made directly from the correlograms of Figure 3. The correlograms produced by the filtered references are shown in Figures 6(a) and 6(b). With no noise added to the scene image, the highway and truck targets were detected with correlation SNRs of 17.3 db and 23.3 db respectively. This represents an improvement of about 9 db over the performance of the correlation measure (3) using unfiltered references.

For a large class of natural imagery, the bulk of the image energy lies in the low spatial frequency region. Hence, the high-pass filters defined for the highway and truck images in the absence of noise would, in the presence of white (uncorrelated) noise, lead to correlation in frequency regions of low signal-to-noise ratio. The uncorrelated noise can be accounted for by adding the noise variance to the diagonal elements of the correlation matrix Σ. The inverse of the exponential approximation to the Σ matrix (with noise included) now no longer corresponds to convolution with a spatially compact 3 x 3 operator, as was the case in the absence of noise.

Some success was obtained in the case of noise, however, using N x N operators constructed from center rows of computed inverse N^2 x $N^2$ correlation matrices. For example, a 5 x 5 operator is obtained as a 5 x 5 arrangement of the thirteenth (center) row of a 25 x 25 inverse correlation matrix. Appendix A lists the 5 x 5, 7 x 7, and 9 x 9 whitening operators for the highway and truck targets corresponding to an image SNR of 10 db. For these operators, the exponential approximations to the correlation matrices were used.

The 9 x 9 operators produced the correlograms shown in Figures 6(c) and 6(d). The highway and truck targets were detected in the presence of 10 db noise with correlation SNRs of 11.1 db and 18.6 db respec-

tively. Since the performances of the 5 x 5 and 7 x 7 operators were within 1 db of that of the 9 x 9 operators, investigation of larger operators was not pursued.

Reference [11] presents a filter, similar to that described in [10], that is obtained from the statistics of both the scene and the target images. Each image vector is whitened by the inverse of one of equal factors of its covariance matrix. That is,

$$\hat{\underline{W}} = A^{-1} \underline{W}$$

$$\hat{\underline{S}}_{uv} = B^{-1} \underline{S}_{uv}$$

where AA^T and BB^T are the covariance matrices of $\underline{W}$ and $\underline{S}_{uv}$ respectively. These filters can be combined into one filter $\Sigma^{-1} = (AB^T)^{-1}$ acting on reference $\underline{W}$. In the case where a stationary or slow-moving target has been extracted from the same scene as that being searched (as in the tracking problem, for example) the A and B are of similar form and the filter is the same as that of reference [10].

The experimental results of this section on the highway and truck photographs illustrate the general necessity of image preprocessing in obtaining adequate detectability using mathematical correlation. As previously pointed out, the reason for this is that the simple correlation-detector (matched filter) is a design for extracting a signal from an uncorrelated noise background. It fails when the background is correlated, or worse still, correlated with the signal itself, as is the case with natural imagery.

The preprocessing filters given in [10] and [11] are applied to the reference image and hence need only be done once. However, the filters are image-dependent. Therefore, unless the target class is sufficiently restricted, the task of determining the required filter must be assigned to the tracking system.

3.0   THE SEQUENTIAL SIMILARITY DETECTION ALGORITHM

The correlation techniques reviewed in the previous section
perform the same volume of computation at each candidate point of regis-
tration (image match-up). Another technique, called the sequential sim-
ilarity detection algorithm (SSDA) [1], greatly reduces the computation
at points of misregistration. Thus, since most of the search points are
points of gross misregistration, the overall computation is drastically
reduced.

For each reference-candidate pair, the SSDA considers the ab-
solute errors of the elements:

$$\epsilon_{uv}(i,j) = |S_{uv}(i,j) - W(i,j)|.$$

The algorithm accumulates the errors, taking the elements in random
order so as to generate new information at each step. As the cumulative
error is computed, it is tested against a threshold, which, when ex-
ceeded, halts the comparison. The number of tests at this point is re-
corded as the measure of similarity $I(u,v)$. $I(u,v)$ is large at points
of near or exact registration, where a large number of tests are re-
quired to cross the threshold.

The cumulative error is a monotonically increasing function.
The threshold is also a monotonically increasing sequence that follows
the expected cumulative error at registration with a margin of safety.
The effect of such a threshold sequence is to terminate testing at mis-
registration early and allow testing at registration to proceed fully.

Reference [1] gives two threshold sequences based on image
degradation due to uncorrelated noise. One sequence, the mean-devia-
tion threshold, considers only the mean and standard deviation of the
noise. This sequence is

$$T(k) = \bar{n}k + \sigma\sqrt{k}$$

where $\bar{n}$ is the mean of the absolute value of the noise and σ is the desired deviation to be accounted for. The form of this sequence is based on the fact that at test k, the accumulated absolute error at registration has a mean of $k\bar{n}$ and a deviation of $\sqrt{k}$ times the deviation of the absolute value of the noise.

A second threshold is derived by assigning for every test the same probability that the threshold is exceeded given that the error has been below threshold up to that point. The equiprobable threshold sequence given in [1] was obtained assuming an exponentially distributed noise.

Since the SSDA performs a nonlinear operation, analysis is difficult. Neither the mean-deviation nor the equiprobable threshold sequences were derived to optimize a performance criterion. In this Report, the SSDA is applied to binary images. This leads to an attractively simple hardware implementation, as proposed in the next section. Threshold sequences are derived and evaluated in Section 5.0, and tests on the highway and truck images are presented in Section 6.0.

4.0   HARDWARE IMPLEMENTATION OF THE SSDA

The remainder of this Report studies the application of
the SSDA to binary images. Because the images are binary, the absolute
errors of the elements are also binary, and the cumulative error is a
monotonically increasing integer-valued sequence whose rate of increase
is never greater than unity. Hence, the threshold sequence, which will
also be a monotonically increasing integer-valued sequence, can be re-
presented as the cumulative sum of a string of binary digits. This
allows the heart of the SSDA correlater to be simply an up/down binary
counter, where the absolute errors are counted up and the threshold se-
quence is counted down. A threshold crossing is signalled by a positive
or zero counter value.

A general hardware configuration for tracking is illustrated
in Figure 7. A charge-coupled device (CCD) imager serves to collect the
imagery [12, 13, 14]. The CCD imager is particularly suited to digital
control in that the video is scanned   by applying pulse rather than ramp
waveforms (as in the vidicon). A gate generator, governed by digital X-Y
position inputs, acts as an electronic gimbal and extracts an L x L
search scene S. The video is digitized to two levels, 0 or 1, by an
analog comparator whose other input is a stored dc signal corresponding
to the mean value of the target image. (This signal can be obtained from
a single detector whose field of view corresponds to the target.) The
resulting binary image is loaded into the random access S memory.
The random access W memory stores the M x M reference target image and
is similarly loaded at initiation of tracking. Following acquisition
of the scene, the SSDA correlator generates the correlation map I(u,v).
The location of the peak of this map is used to update the X-Y input to
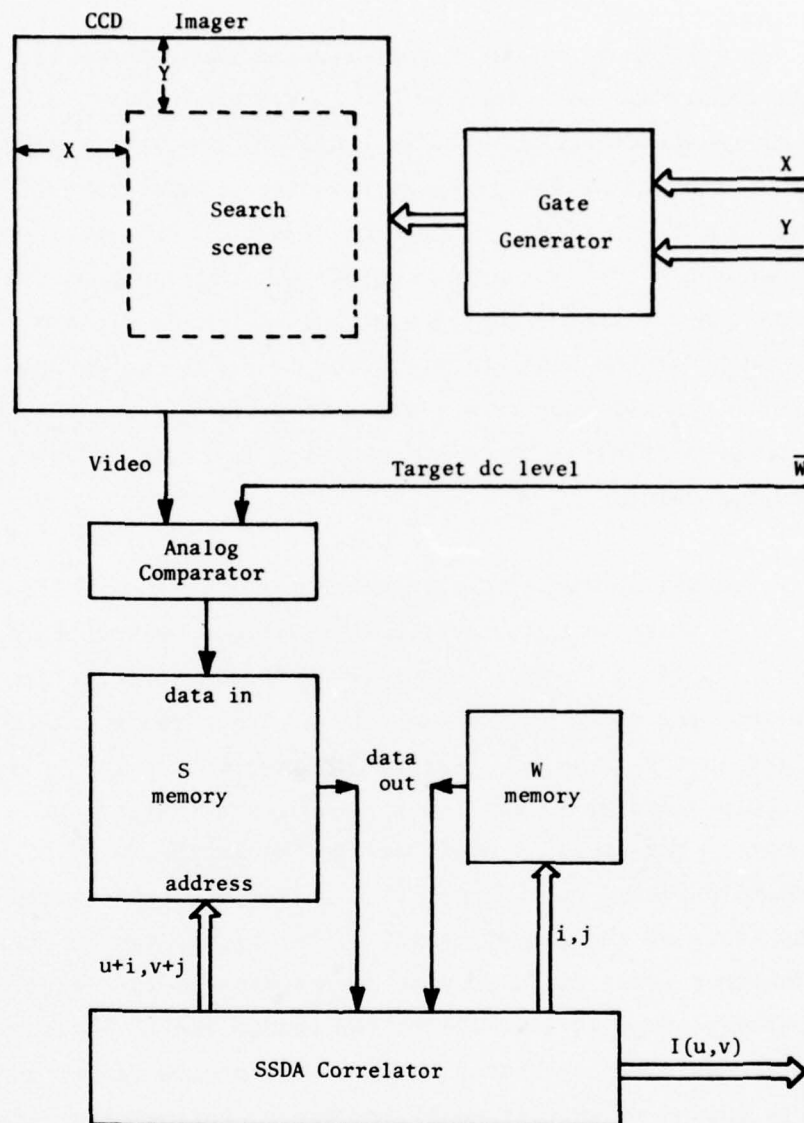the gate generator so as to maintain the target in the center of the
search scene.

Figure 7 - Hardware SSDA tracking configuration

Figure 8 shows a diagram of the correlator for $M = 16$ and $L = 48$. A read-only memory (ROM) and modulo-256 counter generate a random non-repeating sequence of indices i,j that address the S and W memories. The effective address to the S memory is $u + i$, $v + j$, where u and v are obtained from two modulo 33 counters connected in tandem. (Note that here u and v range from 0 to 32 rather than from -16 to +16.) The data from these memories are routed to an exclusive-or (XOR) gate to produce the error signal

$$\varepsilon_{uv}(i,j) \equiv \left| S_{uv}(i,j) - W(i,j) \right|$$

$$= S_{uv}(i,j) \cdot \overline{W(i,j)} + \overline{S_{uv}(i,j)} \cdot W(i,j) \tag{5}$$

where the right-hand side of (5) is a Boolean expression. The modulo 256 counter also addresses another ROM containing the threshold sequence. The threshold and error sequences are combined in logic so that, in the error-threshold counter, errors are counted up, threshold increments are counted down, and no count is generated when an error up-count cancels a threshold down-count. At threshold crossing (detection of zero or positive sign of the error-threshold counter), the following action is taken: the clock ϕ_1 is stopped, the modulo 256 counter value is recorded as $I(u,v)$, the u-v counter is incremented, and the process is repeated.

The processing speed can be maximized by standard techniques such as pipelining, memory-cycle overlap, and parallel processing. In particular, in order to process S_{uv} for n values of v in parallel, it is only necessary to segment the S memory into n banks and install n error-threshold counters plus associated logic within the correlator.

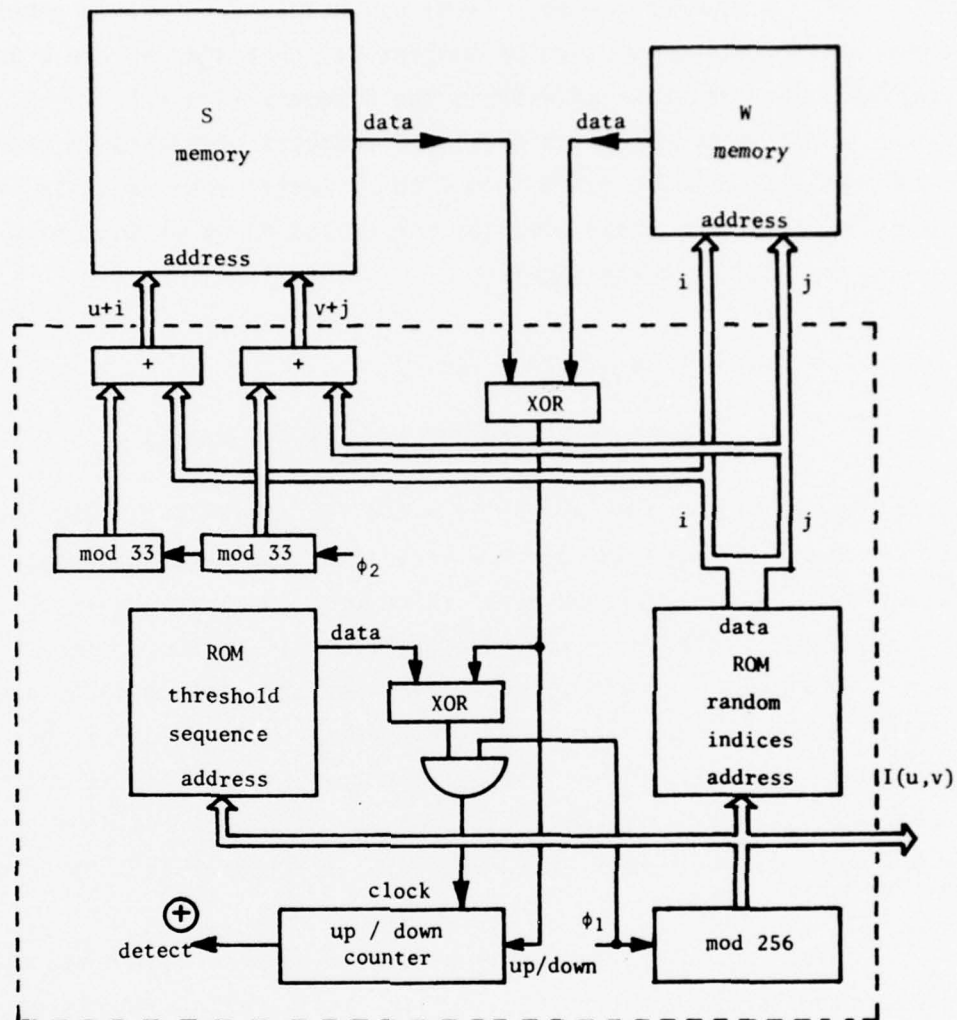It remains to derive the threshold sequences. This will be presented in the next section.

Figure 8 - Diagram of SSDA correlator

5.0   THRESHOLD DERIVATION AND EVALUATION

5.1   Threshold Derivation

In a tracking situation, the error between the scene and the reference image at registration is generally noise. Therefore, in deriving a threshold sequence, it is necessary to consider the statistics of the noise. In the case of binary images, the absolute error $\varepsilon_{uv}(i,j)$ is also binary. The probability density of $\varepsilon_{uv}(i,j)$ consists of impulses at 0 and 1. Letting the error at registration be denoted by $\varepsilon_{00}(i,j)$ and q be the probability that $\varepsilon_{00}(i,j) = 1$, then the mean of $\varepsilon_{00}(i,j)$ is

$$\overline{\varepsilon_{00}(i,j)} = 0 \cdot (1-q) + 1 \cdot q = q$$

The mean-deviation threshold sequence is therefore

$$T(k) = qk + \sigma\sqrt{k} \tag{6}$$

where σ is chosen to provide the desired reliability. Since only integral values of threshold are meaningful, the threshold defined by (6) is rounded up to the next integer. Note that in the hardware implementation of the SSDA as proposed in the previous section, it is the discrete derivative of the threshold that must be stored in the ROM. The error-threshold counter performs the required integration.

The derivation of the equiprobable threshold sequence is much more involved. Let p be the probability that no threshold crossing occurs at any test k, given that none occurred before that test. Then,

$$p \equiv P(\text{no threshold crossing at test k}$$
$$\underline{\text{given}} \text{ no crossing before test k})$$

$$= \frac{P(\text{no crossing until and including test k})}{P(\text{no crossing until and including test k} - 1)}$$

$$= \frac{F_k}{F_{k-1}}$$

where $F_k \equiv P$(no crossing until and including test k). Then the required F_k are $F_k = p^k$. The F_k are obtained for any threshold by calculating the probability density of the cumulative error at every test. Referring to Figure 9, the circles are locations of possible values of the cumulative error for the first few tests. The $f_{m,n}$ within the circles are the probabilities that the cumulative error at test m is n. At each test, the cumulative error can increase by one with probability q, or remain the same with probability 1-q. Thus,

$$f_{m,n} = (1-q) \, f_{m-1,n} + q \, f_{m-1, \, n-1}$$

$$f_{m,0} = (1-q) \, f_{m-1,0}$$

$$f_{m,m} = q \, f_{m-1, \, m-1}$$

The calculation of the $f_{m,n}$ proceeds from left to right (increasing m). At each test, the $f_{m,n}$ in circles on or above the threshold are immediately set to zero since the objective is to compute for paths that do not hit threshold. The probabilities F_k are then given by $\sum_{n=0}^{k} f_{k,n}$. Since the required F_k were p^k for the equiprobable threshold, the threshold T(k) can be found individually (but in strictly ascending order) by trial and error so as to obtain as closely as possible the required F_k. Since the threshold is a monotonically increasing sequence but increases at a maximum rate of one per test, the maximum number of trials required is two per test.

Typical threshold sequences of both mean-deviation and equiprobable types will be presented later, following a discussion of their performance comparison.
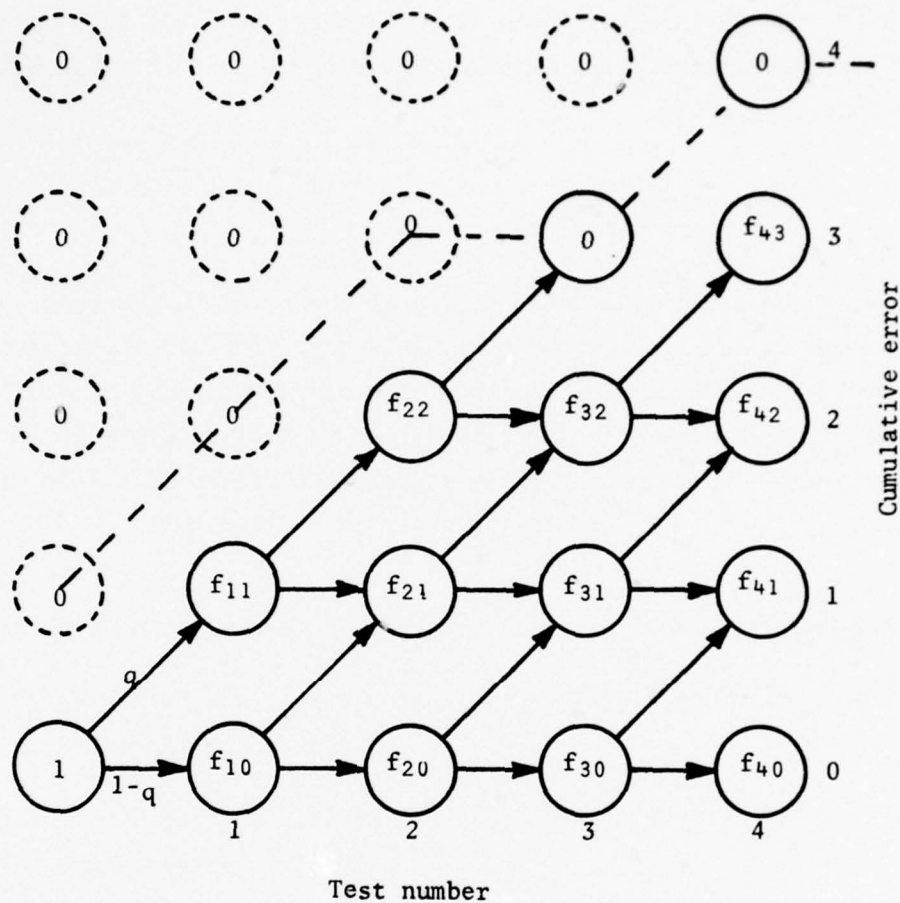
Figure 9 - Diagram for computation of $F_k \equiv P$(no threshold crossing until and including test k) by calculating the probability density of the cumulative error: $f_{m,n}$ = probability that cumulative error is n at test m. F_k is given by $\sum_j f_{k,j}$

5.2 Performance Evaluation

The remainder of this section presents an analytical evalua-
tion of the two threshold sequences just derived. For this purpose,
the performance criterion is taken to be the signal-to-noise ratio of
the correlation map

$$SNR = \frac{E[I(0,0)]}{(E[I^2(u,v)])^{\frac{1}{2}}}$$

which is the ratio of the expected peak to the rms background. An ap-
proximate calculation of the first and second moments involved here
requires the probability density of $I(u,v)$ for three regions of interest:
gross misregistration, near registration, and exact registration. These
regions are handled by assigning appropriate values of q (the probability
that $\varepsilon_{uv}(i,j) = 1$). The densities are then given by

$$P(I(u,v)=k) = P(\text{threshold crossing at test k } \underline{and} \text{ none before k})$$

$$= P(\text{crossing at test k } \underline{given} \text{ none before}) \cdot$$
$$P(\text{no crossing before test k})$$

$$= [1 - P(\text{no crossing at test k } \underline{given} \text{ none before})] \cdot$$
$$P(\text{no crossing before test k})$$

$$= \left[1 - \frac{P(\text{no crossing at or before k})}{P(\text{no crossing before test k})}\right] \cdot$$
$$P(\text{no crossing before test k})$$
$$= [1 - \frac{F_k}{F_{k-1}}] \, F_{k-1}$$

$$= F_{k-1} - F_k$$

where the F_k are defined and obtained as previously described.

In assigning the proper values of q for the various regions
of the correlation map, the scene and reference images are assumed to

have a uniform histogram. The noise is taken to be exponentially distributed with the following distribution: $f(x) = \frac{1}{2\lambda} e^{-x/2\lambda}$, where x is a random noise variable. At exact registration,

$$\epsilon_{00}(i,j) = 1 \text{ if } x > \overline{W} - W_{ij} \text{ for } W_{ij} < \overline{W}$$

$$\text{or } x < \overline{W} - W_{ij} \text{ for } W_{ij} > \overline{W}$$

$$= 0 \text{ otherwise}$$

This leads to $q \equiv p(\epsilon_{00}(i,j)=1) = \lambda(1-e^{-1/2\lambda})$. At gross misregistration, $\epsilon_{uv}(i,j)$ is taken to be 0 or 1 with equal probability; hence, q = 0.5. At near registration, it was found experimentally from the highway and truck scenes that for moderate image SNRs, q = 0.2, 0.3, and 0.4 for locations that are respectively 1, 2, and 3 elements away from exact registration.

It remains to establish a basis of comparison to determine, for any value of λ, what p of the equiprobable threshold should correspond to what σ of the mean-deviation threshold. This basis was chosen to be that of equal detection rate, which is arbitrarily defined here as the probability that the correlation peak is greater than or equal to half the maximum of 256; that is, $P(I(0,0) > 128)$ should be the same for both thresholds. This probability is given by F_{128}. The rationale behind this type of criterion is that there must be some lower limit for the correlation peak below which the tracking system will have to decide not to accept the result and to switch to a higher threshold corresponding to a higher noise level. This lower limit was chosen to be 128. A peak of less than 128 using the correct threshold is therefore considered an error since it will incorrectly raise the threshold. A decision to lower the threshold (corresponding to a lower noise level) follows the occurrence of saturation, a situation where more than one correlation point reaches the maximum.

Figure 10 illustrates the mean-deviation and equiprobable threshold sequences for four image SNRs (four values of λ) and for two detection rates, 0.99 and 0.999, and Figure 11, the predicted correlation SNRs. Figure 12 shows the F_k sequences at registration for both types of threshold for an image signal-to-noise ratio of 10 db and a detection rate of 0.999. The shapes of these F_k sequences are typical for all the signal-to-noise ratios and detection rates considered.

It is evident from Figure 11 that, at a detection rate of 0.99, the mean-deviation threshold enjoys a higher correlation SNR than the equiprobable threshold, except at the low image SNR of 10 db. This advantage is considerably reduced at a detection rate of 0.999, where the equiprobable threshold is superior at both 10 db and 15 db image SNRs.

An explanation for this can be found on examination of Figures 10 and 12. Comparison of Figures 10(a) with 10(b) and 10(c) with 10(d) indicates that the mean-deviation sequences are initially lower and terminally higher than the corresponding equiprobable sequences. This corresponds with Figure 12, where the F_k of the mean-deviation sequence drops much more rapidly at the beginning but levels off toward the end. At low noise levels, most of the misregistration points, including near registration, terminate very early resulting in a signal-to-noise advantage to the mean-deviation sequence. At high noise levels, however, the q at exact registration begins to approach that of near registration and, therefore, the sequence that has higher terminal values is heavily penalized at points of near registration. It is for this reason that the performance of the mean-deviation threshold declines more rapidly with increasing noise level and with increasing detection rate. Ultimately the mean-deviation sequence will be more susceptible to saturation, where some of the near registration points will reach maximum as well as the exact registration point.

a) Mean-deviation threshold,
detection rate = 0.99

b) Equiprobable threshold,
detection rate = 0.99

c) Mean deviation threshold,
detection rate = 0.999

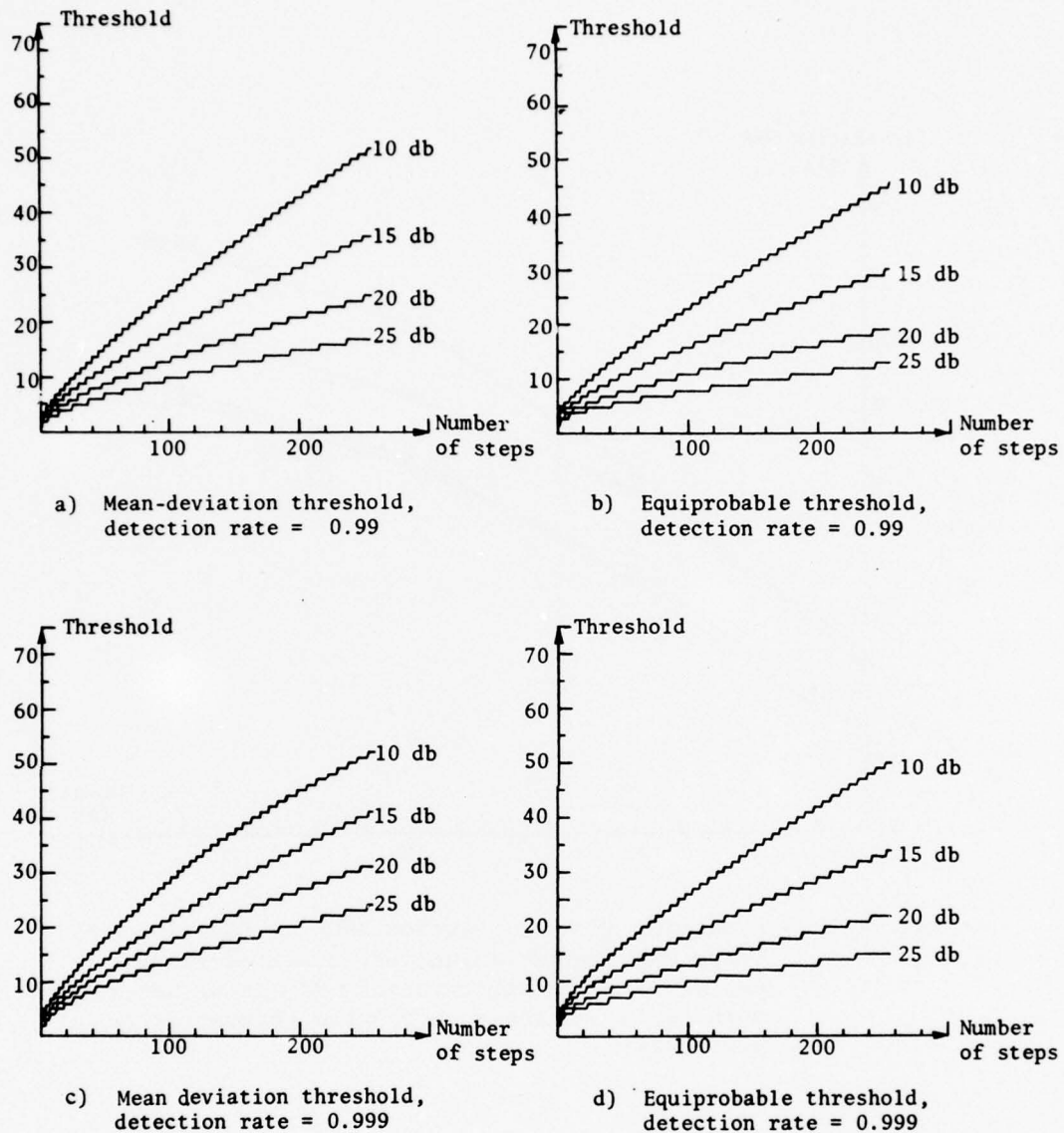d) Equiprobable threshold,
detection rate = 0.999

Figure 10 - Mean deviation and equiprobable thresholds for four values
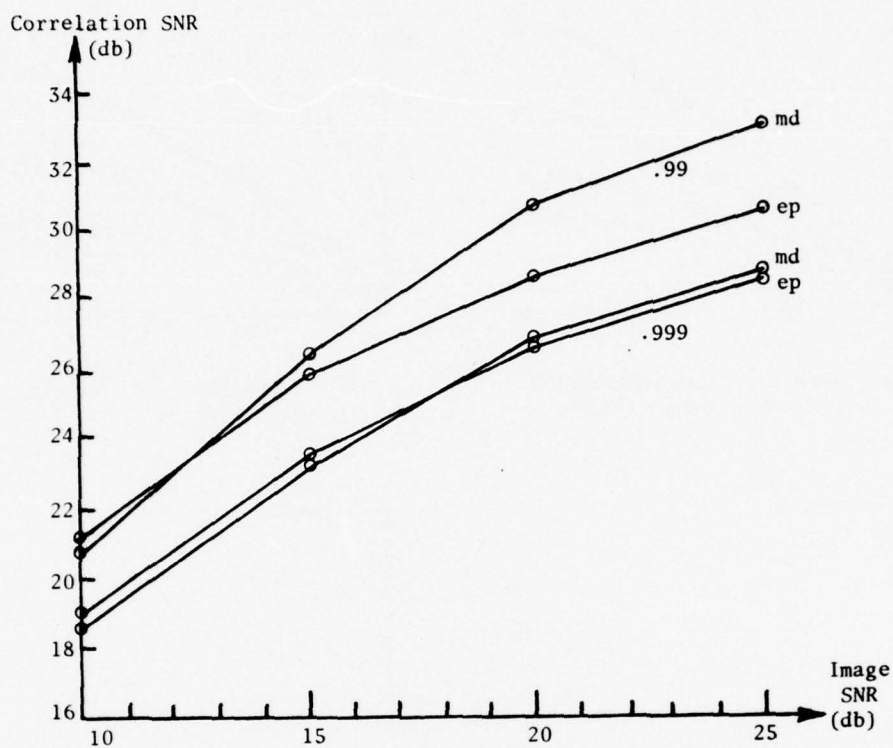of image SNR

Figure 11 - Predicted SSDA correlation SNRs as functions of
image SNR for two values of detection rate, 0.99
and 0.999. The abbreviations md and ep designate
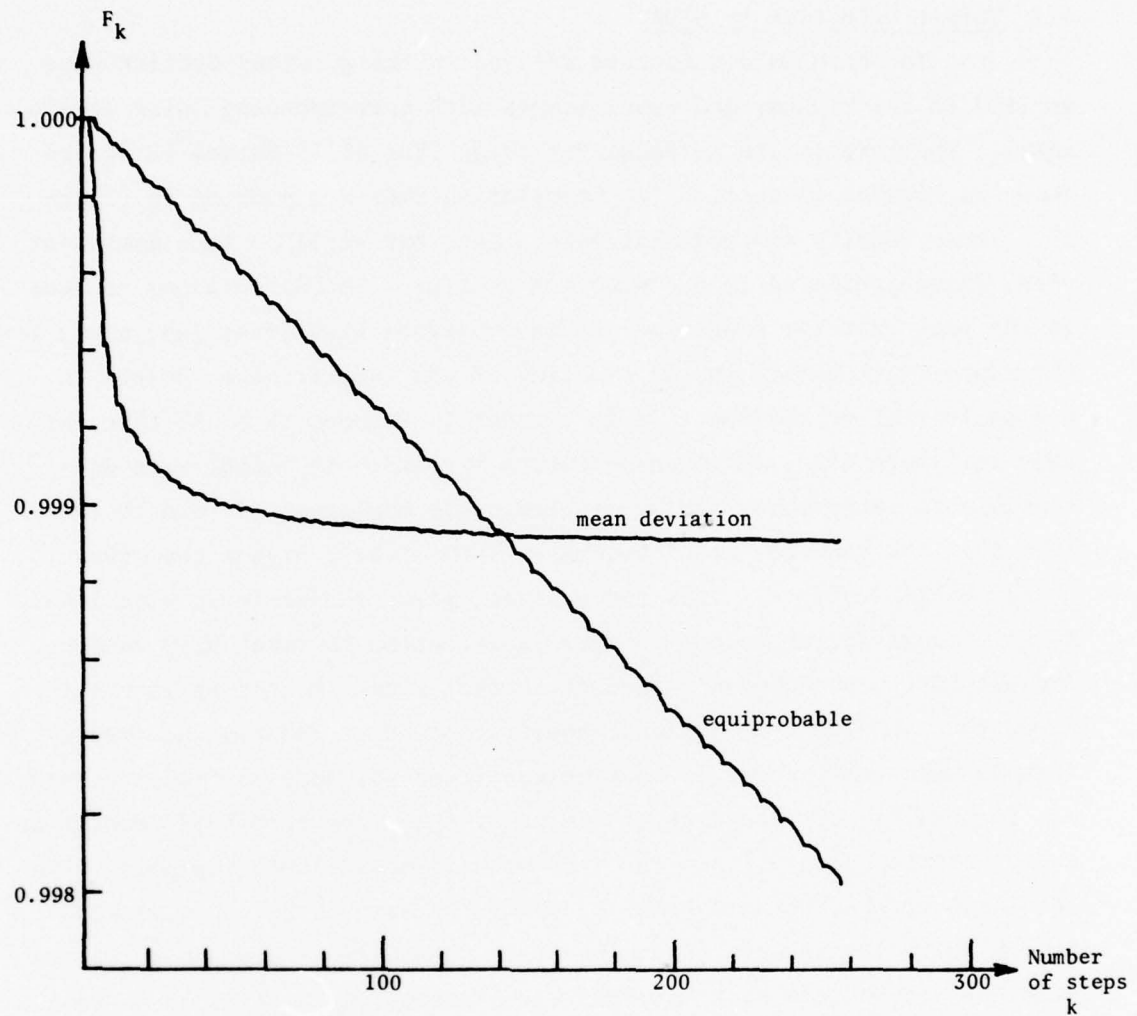mean-deviation and equiprobable thresholds res-
pectively

Figure 12 - F_k sequences for mean deviation and equiprobable thresholds corresponding to 10 db image SNR and 0.999 detection rate

6.0 EXPERIMENTAL RESULTS

6.1 Target Detection by SSDA

The threshold sequences derived in the previous section were applied to the highway and truck images with corresponding noise levels added. The correlation surfaces for image SNRs of 25 db and 10 db are shown in Figures 13 to 16. The correlation SNRs are plotted in Figure 17. These results are somewhat lower than, but still in some agreement with, those predicted in the previous section. The differences are due to the fact that the images do not have uniform histograms and, also, to the approximate nature in the handling of near-registration points in the analytical evaluation. It is evident in Figures 13 to 16 that, at very low image SNRs, the mean-deviation threshold is rather more susceptible to saturation. This, as previously explained, is due to the fact that the mean-deviation sequence is terminally higher than the equiprobable sequence. Thus the mean-deviation threshold is more likely to allow correlation points of near registration to reach high values. *The saturation phenomenon is not disastrous since the target is still* detected. It should be avoided, however, since it reduces the resolution to which the target is locatable. (Even so, some sort of recovery may be possible by recording the value of the error-threshold counter at every point of saturation. The true peak is most likely the point with the least error-threshold count.) Using the mean-deviation threshold at low noise levels and the equiprobable threshold at high noise levels seems to provide the most satisfactory performance in terms of correlation signal-to-noise ratio and resistance to saturation.
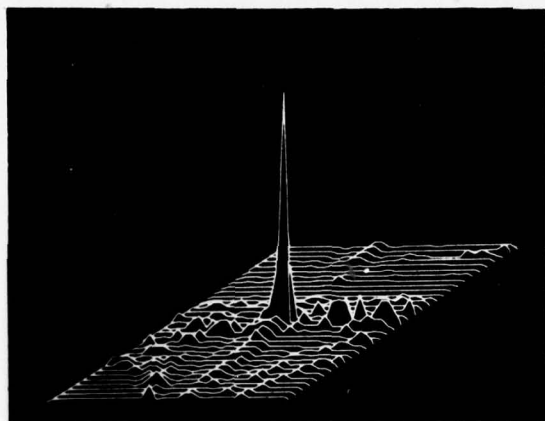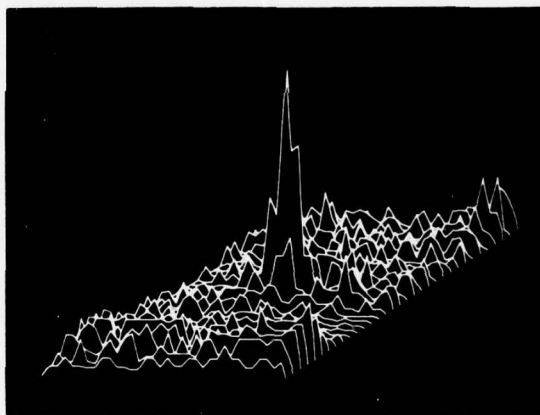
(a) Highway correlogram
     Image SNR = 25 db
     Correlation SNR = 32.4 db
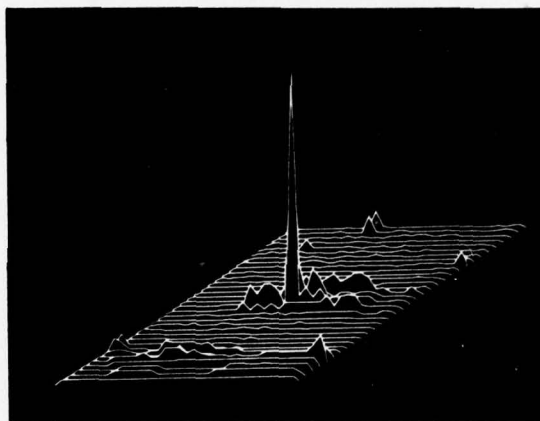
(b) Truck correlogram
     Image SNR = 25 db
     Correlation SNR = 31.7 db
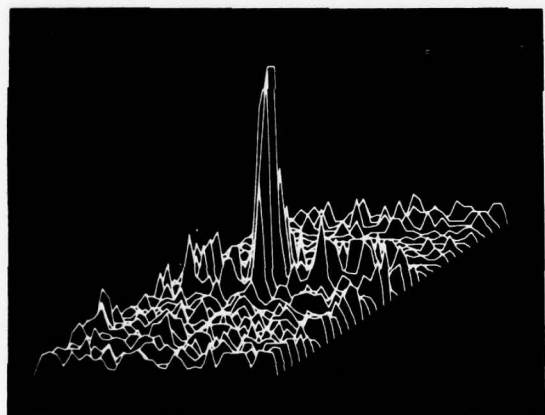
(c) Highway correlogram
     Image SNR = 10 db
     Correlation SNR = 20.8 db

(d) Truck correlogram
     Image SNR = 10 db
     Correlation SNR = 20.8 db

Figure 13 - SSDA correlograms with mean deviation threshold,
detection rate = 0.99

(a)   Highway correlogram
Image SNR = 25 db
Correlation SNR = 29.2 db

(b)   Truck correlogram
Image SNR = 25 db
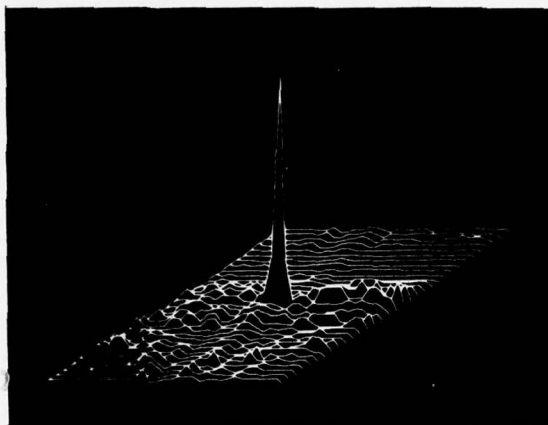Correlation SNR = 29.6 db

(c)   Highway correlogram
Image SNR = 10 db
Correlation SNR = 21.2 db

(d)   Truck correlogram
Image SNR = 10 db
Correlation SNR = 20.7 db

Figure 14 - SSDA correlograms with equiprobable threshold,
detection rate = 0.99

(a) Highway correlogram
Image SNR = 25 db
Correlation SNR = 26.6 db

(b) Truck correlogram
Image SNR = 25 db
Correlation SNR = 26.5 db

(c) Highway correlogram
Image SNR = 10 db
Correlation SNR = 18.1 db

(d) Truck correlogram
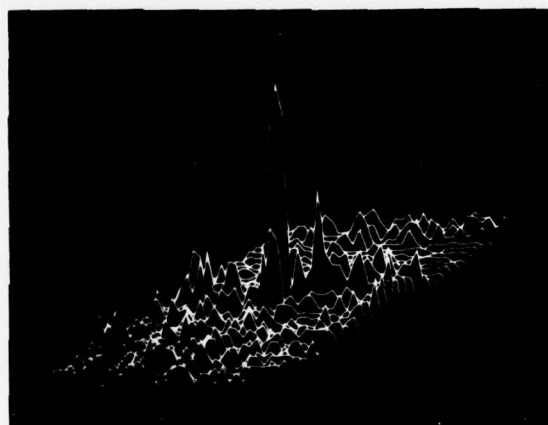Image SNR = 10 db
Correlation SNR = 17.6 db

Figure 15 - SSDA correlograms with mean deviation threshold,
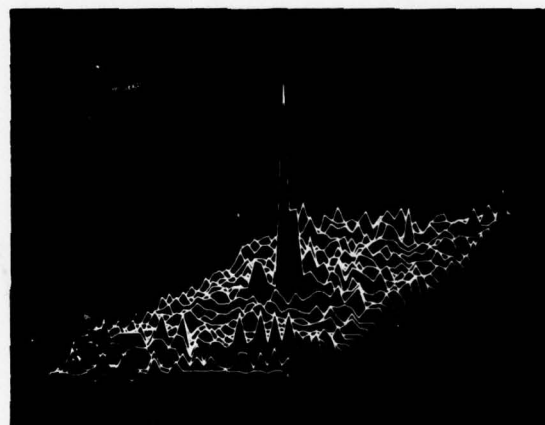detection rate = 0.999
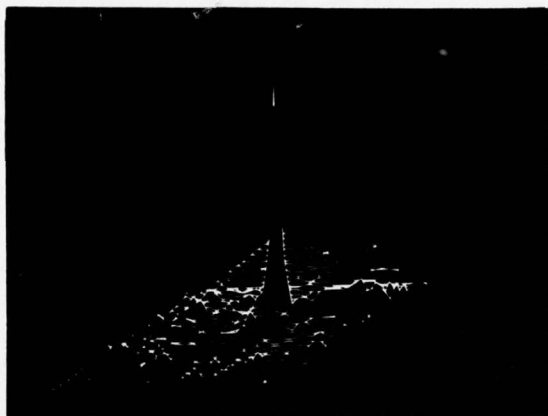
(a) Highway correlogram
Image SNR = 25 db
Correlation SNR = 27.3 db

(b) Truck correlogram
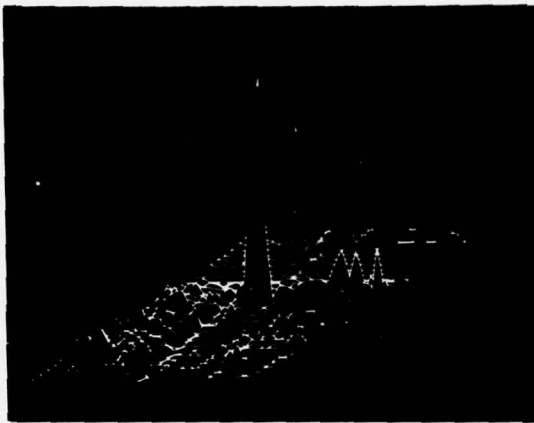Image SNR = 25 db
Correlation SNR = 27.1 db
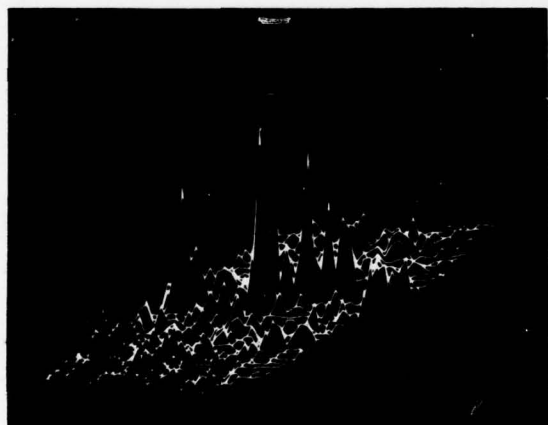
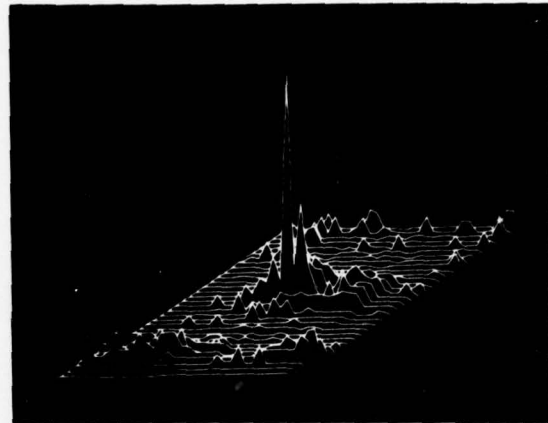(c) Highway corelogram
Image SNR = 10 db
Correlation SNR = 18.6 db
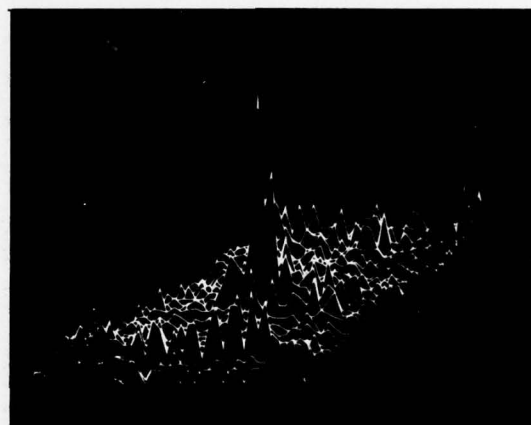
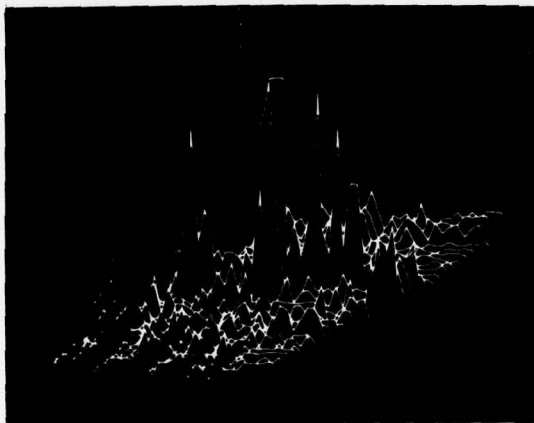(d) Truck correlogram
Image SNR = 10 db
Correlation SNR = 18.2 db

Figure 16 - SSDA correlograms with equiprobable threshold,
detection rate = 0.999

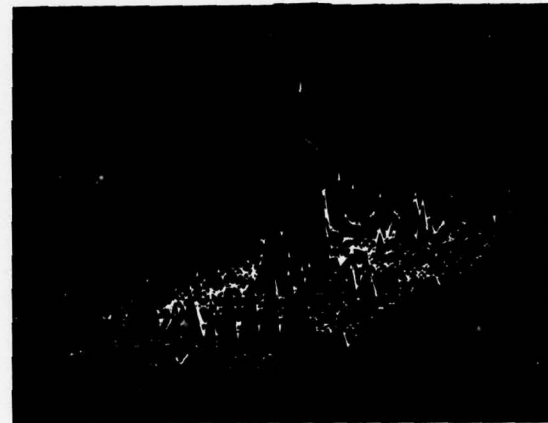Figure 17 - Experimental SSDA correlation SNRs for highway and
truck targets as a function of image SNR for two
values of detection rate, 0.99 and 0.999. The abbre-
viations md and ep designate mean-deviation and equi-
probable thresholds respectively.

6.2 Image Preprocessing for the SSDA

A natural question to be asked at this point is how filtering prior to binarization can improve the SSDA's performance, particularly at low image SNRs. In the optimization of a filter, it is desirable to sharpen the correlogram by decorrelating the image without excessively 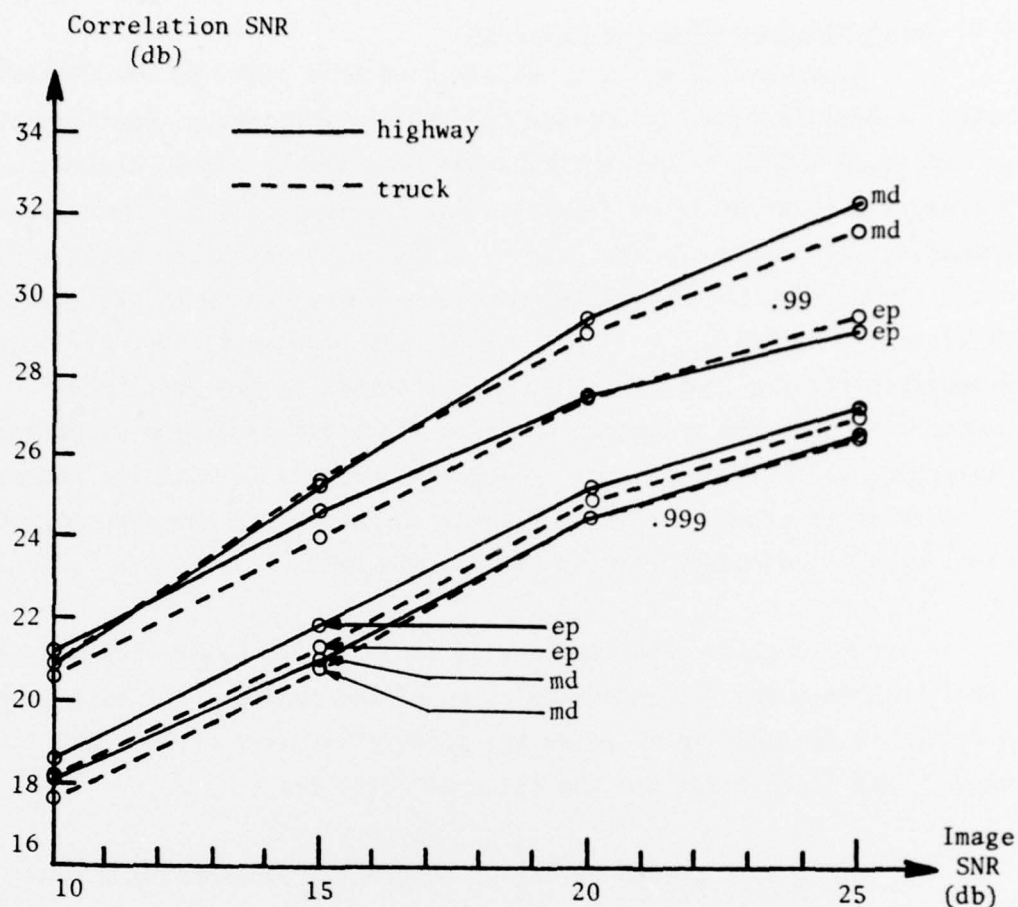enhancing the noise. In the case of classical correlation, this is a tractable problem and analytical solutions are given by the filters of References [10] and [11]. For the SSDA, the problem is very difficult because of the nonlinearity. A highly interesting prospect here, however, is that the reduction of noise alone may produce a significant sharpening of the correlogram. The basis for this is that the reduction in noise would allow the use of a lower threshold for the same detection rate, with a consequent gain in correlation SNR.

The problem then consists in reducing the noise without significantly broadening the autocorrelation of the images. For this purpose, a filter is designed to minimize the integral squared error (ISE) between the clean image and the filtered noisy image.

Let $\underline{S}$ be a column vector of length M^2 representing a row-scanned M x M image S. Assume that the imaging sensor gives $\underline{S} + \underline{N}$, where $\underline{N}$ is an independent zero mean noise vector of length M^2. Let the filtered image vector be given by

$$\hat{\underline{S}} = H(\underline{S} + \underline{N})$$

where H is an M^2 x M^2 filter matrix. The ISE is then given by

$$\overline{\Sigma e^2} = E[(\underline{S} - H(\underline{S} + \underline{N}))^T (\underline{S} - H(\underline{S} + \underline{N}))]$$

$$= E[\underline{S}^T\underline{S} - \underline{S}H^T\underline{S} - \underline{N}^TH^T\underline{S} - \underline{S}^TH\underline{S}$$

$$- \underline{S}^TH\underline{N} + \underline{S}^TH^TH\underline{S} + \underline{N}^TH^TH\underline{S} + \underline{S}^TH^TH\underline{N} + \underline{N}^TH^TH\underline{N}]$$

$$= E[\underline{S}^T\underline{S} - \underline{S}^TH^T\underline{S} - \underline{S}^TH\underline{S} + \underline{S}^TH^TH\underline{S} + \underline{N}^TH^TH\underline{N}]$$

where cross-terms are dropped because $\underline{N}$ is zero-mean and independent of $\underline{S}$. By interchanging the expectation operator with a differentiation operator (with respect to H), a straightforward minimization of the ISE is given by

$$H = \Sigma_s (\Sigma_s + \Sigma_n)^{-1}$$

where

$\Sigma_s = E[\underline{S}\ \underline{S}^T]$ is the image correlation matrix.

$\Sigma_n = E[\underline{N}\ \underline{N}^T]$ is the noise covariance matrix.

This filter is the same as that given in Helstrom [15]. It was obtained by minimizing the mean squared error:

$$MSE = \text{Trace } E\left[(\underline{S} - H(\underline{S} + \underline{N}))(\underline{S} - H(\underline{S} + \underline{N}))^T\right].$$

Assumption of zero-mean uncorrelated noise leads to the representation of Σ_n by $\sigma^2 I$, where σ^2 is the noise variance and I is the $M^2 \times M^2$ identity matrix.

In practical application, operators for convolution are extracted from H using the technique presented in Section 2.0 for the whitening filters. Appendix β gives the 5 x 5, 7 x 7, and 9 x 9 noise-reduction operators for the highway and truck targets corresponding to a 10 db image SNR. For the image correlation matrix Σ_s, the same exponential approximation of Section 2.0 was used.

It was determined experimentally that all the operators listed in Appendix B reduce the noise in the highway and truck images by about 15 db. This allows the use of thresholds that correspond to 25 db rather than 10 db image SNR. The SSDA correlograms produced by the 9 x 9 operators, using equiprobable threshold, are shown in Figures 18(a) and 18(b). These correlograms should be compared with those of

Figures 14(c) and 14(d) where no filtering was applied. The correlation
SNR improvements are 6.6 db and 4.4 db for the highway and truck targets
respectively. Again, the performances of the 5 x 5 and 7 x 7 operators
were within 1 db of that of the 9 x 9 operator.

6.3 Comments

The highway and truck correlograms presented in Section 2.0 and
in this section indicate that on the basis of performance alone, the
SSDA is highly competitive with the mathematical correlation technique.
The performance of the SSDA is obtained, however, with a good deal less
effort. Prefiltering of the images is not a requisite, although improved
performance at high noise levels can be obtained by filtering for noise
reduction. The correlograms are generated with simple and considerably
less computation. This feature makes the SSDA highly attractive as the
basis of a hardware correlation tracking system.
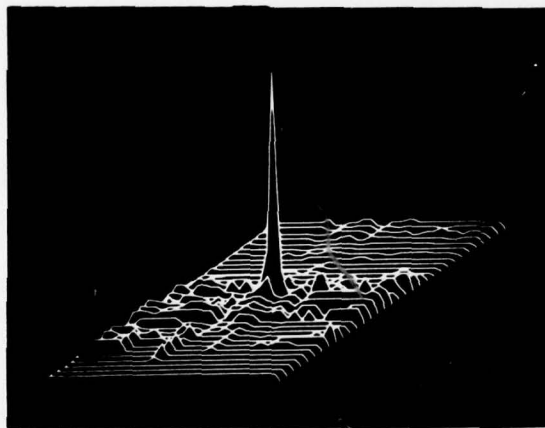
(a) Highway correlogram
     Correlation SNR = 27.8 db
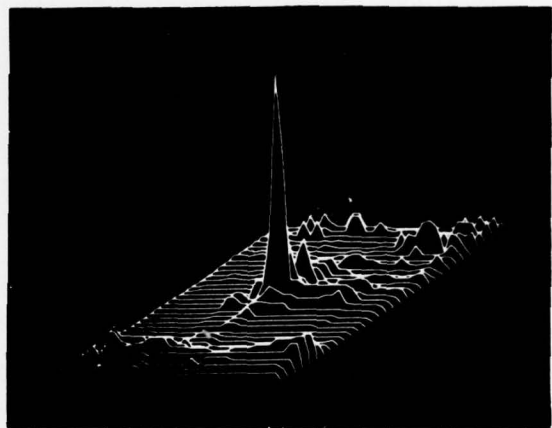
(b) Truck correlogram
     Correlation SNR = 25.1 db

Figure 18 - SSDA correlograms with filtered images having 10 db
            SNR Before filtering. The filters are 9 x 9 convo-
            lution operators designed for minimum integral squared
            error. The equiprobable threshold with 0.99 detection
            rate was used.

7.0 CONCLUSION

Two classes of digital image correlation techniques have been reviewed with a view to application to area correlation tracking. Tests on photographs of a highway and a military truck demonstrate the requirement of image preprocessing to obtain adequate target detectability using the mathematical correlation method. The preprocessing is of a high-pass filter type intended to decorrelate the rather highly correlated target images. This whitening of the target images must be compromised in the presence of uncorrelated noise, however, in order to avoid correlating in frequency regions of low signal-to-noise ratio.

The second technique, the sequential similarity detection algorithm (SSDA), proved to be very effective without any image preprocessing. Applied to binary images, this technique leads to a very simple hardware implementation, for which a suggested configuration is given in this Report. Two threshold sequences for the SSDA were derived, evaluated and tested. It was found that the mean-deviation threshold was more effective at high image SNR, while the equiprobable threshold was preferable at low SNR. At high noise levels, filtering for reduction of noise produces improved correlation SNR by allowing the use of lower thresholds.

The simplicity of the SSDA, together with its success in detecting targets in still photographs, encourages further work on this technique. For this purpose, a simulated tracking configuration is to be set up using a television camera and a mini-computer. Of special interest will be the determination of the algorithm's sensitivity to magnification and rotation of the search scene.

8.0 ACKNOWLEDGEMENTS

9.0 REFERENCES

1. Barnea, D.I., and Silverman, H.F., "A Class of Algorithms for Fast Digital Image Registration", IEEE Transactions on Computers, Vol. C-21, pp.179-186, February 1972.

2. Cochran, W.T. et al, "What is the Fast Fourier Transform?", Proceedings of the IEEE, Vol. 55, pp.1664-1674, October 1967.

3. Bergland, G.D., "A Guided Tour of the Fast Fourier Transform", IEEE Spectrum, pp.41-52, July 1969.

4. Cooley, J.W., Lewis, P.A.W., and Welch, P.D., "Application of the Fast Fourier Transform to Computation of Fourier Integrals, Fourier Series, and Convolution Integrals", IEEE Transactions on Audio and Electro-acoustics, Vol. AU-15, pp.79-84, June 1967.

5. Preston, K., "Computing at the Speed of Light", Electronics, pp.72-83, September 6, 1965.

6. Vander Lugt, A., "Signal Detection by Complex Spatial Filtering", IEEE Transactions on Information Theory, Vol. IT-10, pp.139-145, April 1964.

7. Rosenfeld, A., "Picture Processing by Computer", Academic Press, New York, 1970.

8. Andrews, H.C., "Computer Techniques in Image Processing", Academic Press, New York, 1970.

9. Anuta, P.E., "Spatial Registration of Multispectral and Multitemporal Digital Imagery Using Fast Fourier Transform Techniques", IEEE Transactions on Geoscience Electronics, Vol. GE-8, pp.353-368, October 1970.

10. Arcese, A., Mengert, P.H., and Trombini, E.W., "Image Detection through Bipolar Correlation", IEEE Transactions on Information Theory, Vol. IT-16, pp.534-541, September 1970.

11. Pratt, W.K., "Correlation Techniques of Image Registration", IEEE Transactions on Aerospace and Electronic Systems, Vol. AES-10, pp.353-358, May 1974.

12. Séquin C.H., and Tompsett, M.F., "Charge Transfer Devices", Academic Press, New York, 1975.

13. Tompsett, M.F., Bertram, W.J., Sealer, D.A., and Séquin, C.H., "Charge-Coupling Improves its Image, Challenging Video Camera Tubes", Electronics, pp.162-169, January 18, 1973.

14. Amelio, G.F., "Charge-Coupled Devices", Scientific American, pp.22-31, February 1974.

15. Helstrom, C.W., "Image Restoration by the Method of Least Squares", Journal of the Optical Society of America, Vol.57, pp. 297-303, March 1967.

APPENDIX   A

The following tables list the 5 x 5, 7 x 7, and 9 x 9 whitening operators for the highway and truck images with a 10 db signal-to-noise ratio. These filters sharpen the correlograms generated by mathematical correlation.

Whitening operators for the highway image

a) 5 x 5 operator

```
 .021  -.000  -.063  -.000   .021
-.000  -.023  -.090  -.023  -.000
-.158  -.184  1.000  -.184  -.158
-.000  -.023  -.090  -.023  -.000
 .021  -.000  -.063  -.000   .021
```

b) 7 x 7 operator

```
 .018   .013  -.004  -.056  -.004   .013   .018
 .018   .013  -.006  -.061  -.006   .013   .018
 .006   .000  -.021  -.080  -.021   .000   .006
-.113  -.122  -.146  1.000  -.146  -.122  -.113
 .006   .000  -.021  -.080  -.021   .000   .006
 .018   .013  -.006  -.061  -.006   .013   .018
 .018   .013  -.004  -.056  -.004   .013   .018
```

c) 9 x 9 operator

```
 .011   .010   .008  -.004  -.048  -.004   .008   .010   .011
 .012   .011   .008  -.005  -.052  -.005   .008   .011   .012
 .013   .012   .008  -.007  -.058  -.007   .008   .012   .013
 .007   .005  -.001  -.019  -.073  -.019  -.001   .005   .007
-.088  -.092  -.101  -.122  1.000  -.122  -.101  -.092  -.088
 .007   .005  -.001  -.019  -.073  -.019  -.001   .005   .007
 .013   .012   .008  -.007  -.058  -.007   .008   .012   .013
 .012   .011   .008  -.005  -.052  -.005   .008   .011   .012
 .011   .010   .008  -.004  -.048  -.004   .008   .010   .011
```

Whitening operators for the truck image

a) 5 x 5 operator

```
  .036    .013   -.112    .013    .036
  .021   -.008   -.148   -.008    .021
 -.162   -.204   1.000   -.204   -.162
  .021   -.008   -.148   -.008    .021
  .036    .013   -.112    .013    .036
```

b) 7 x 7 operator

```
  .018    .018    .007   -.084    .007    .018    .018
  .021    .020    .005   -.097    .005    .020    .021
  .017    .012   -.011   -.129   -.011    .012    .017
 -.112   -.126   -.164   1.000   -.164   -.126   -.112
  .017    .012   -.011   -.129   -.011    .012    .017
  .021    .020    .005   -.097    .005    .020    .021
  .018    .018    .007   -.084    .007    .018    .018
```

c) 9 x 9 operator

```
  .006    .008    .011    .007   -.063    .007    .011    .008    .006
  .009    .010    .012    .005   -.072    .005    .012    .010    .009
  .013    .014    .014    .001   -.088    .001    .014    .014    .013
  .015    .013    .007   -.014   -.119   -.014    .007    .013    .015
 -.082   -.091   -.107   -.144   1.000   -.144   -.107   -.091   -.082
  .015    .013    .007   -.014   -.119   -.014    .007    .013    .015
  .013    .014    .014    .001   -.088    .001    .014    .014    .013
  .009    .010    .012    .005   -.072    .005    .012    .010    .009
  .006    .008    .011    .007   -.063    .007    .011    .008    .006
```

APPENDIX   B

The following listings give the 5 x 5, 7 x 7, and 9 x 9
noise-reduction operators for the highway and truck images with a 10 db
signal-to-noise ratio.   These filters sharpen the SSDA correlograms by
reducing noise and allowing lower thresholds to be used.   They are ob-
tained by a minimization of the integral squared error.

Noise-reduction operators for the highway image

a)   5 x 5 operator

-.017	.000	.050	.000	-.017
.000	.018	.072	.018	.000
.126	.147	.204	.147	.126
.000	.018	.072	.018	.000
-.017	.000	.050	.000	-.017

b)   7 x 7 operator

-.015	-.011	.003	.046	.003	-.011	-.015
-.015	-.010	.005	.050	.005	-.010	-.015
-.005	-.000	.017	.066	.017	-.000	-.005
.093	.100	.120	.174	.120	.100	.093
-.005	-.000	.017	.066	.017	-.000	-.005
-.015	-.010	.005	.050	.005	-.010	-.015
-.015	-.011	.003	.046	.003	-.011	-.015

c)   9 x 9 operator

-.009	-.009	-.006	.004	.041	.004	-.006	-.009	-.009
-.010	-.010	-.007	.004	.044	.004	-.007	-.010	-.010
-.011	-.010	-.006	.006	.049	.006	-.006	-.010	-.011
-.006	-.004	.001	.016	.062	.016	.001	-.004	-.006
.075	.078	.085	.104	.154	.104	.085	.078	.075
-.006	-.004	.001	.016	.062	.016	.001	-.004	-.006
-.011	-.010	-.006	.006	.049	.006	-.006	-.010	-.011
-.010	-.010	-.007	.004	.044	.004	-.007	-.010	-.010
-.009	-.009	-.006	.004	.041	.004	-.006	-.009	-.009

Noise-reduction operators for the truck image

a) 5 x 5 operator

```
        -.027   -.010    .082   -.010   -.027
        -.015    .006    .108    .006   -.015
         .119    .149    .267    .149    .119
        -.015    .006    .108    .006   -.015
        -.027   -.010    .082   -.010   -.027
```

b) 7 x 7 operator

```
     -.014   -.014   -.005    .065   -.005   -.014   -.014
     -.016   -.015   -.004    .075   -.004   -.015   -.016
     -.013   -.009    .009    .099    .009   -.009   -.013
      .086    .097    .126    .232    .126    .097    .086
     -.013   -.009    .009    .099    .009   -.009   -.013
     -.016   -.015   -.004    .075   -.004   -.015   -.016
     -.014   -.014   -.005    .065   -.005   -.014   -.014
```

c) 9 x 9 operator

```
 -.005   -.006   -.009   -.005    .049   -.005   -.009   -.006   -.005
 -.007   -.008   -.010   -.004    .057   -.004   -.010   -.008   -.007
 -.010   -.011   -.011   -.001    .069   -.001   -.011   -.011   -.010
 -.011   -.010   -.006    .011    .094    .011   -.006   -.010   -.011
  .065    .071    .084    .113    .213    .113    .084    .071    .065
 -.011   -.010   -.006    .011    .094    .011   -.006   -.010   -.011
 -.010   -.011   -.011   -.001    .069   -.001   -.011   -.011   -.010
 -.007   -.008   -.010   -.004    .057   -.004   -.010   -.008   -.007
 -.005   -.006   -.009   -.005    .049   -.005   -.009   -.006   -.005
```

CRDV R-4097/77 (NON CLASSIFIE)

Bureau – Recherche et Développement, Ministère de la Défense nationale, Canada.
CRDV, C.P. 880, Courcelette, Qué. G0A 1R0.

"Digital Area Correlation Tracking by Sequential Similarity Detection"
by C. Munteanu

La corrélation d'images est une méthode efficace de poursuivre une cible qui ne possède pas de traits saillants. Ceci implique la détection d'une cible dans son milieu au moyen des similitudes qu'elle a avec une image étalon de la cible. Ce rapport présente une évaluation de la performance de l'algorithme séquentiel pour la détection de la similarité (ASDS) dans la détection numérique d'images. On montre que la performance de l'ASDS est comparable à celle de la méthode courante de corrélation mathématique. Les deux techniques sont décrites et essayées sur des photographies. Une évaluation analytique de l'ASDS appliquée à des images binaires est présentée. (NC)

CRDV R-4097/77 (NON CLASSIFIE)

Bureau – Recherche et Développement, Ministère de la Défense nationale, Canada.
CRDV, C.P. 880, Courcelette, Qué. G0A 1R0.

"Digital Area Correlation Tracking by Sequential Similarity Detection"
by C. Munteanu

La corrélation d'images est une méthode efficace de poursuivre une cible qui ne possède pas de traits saillants. Ceci implique la détection d'une cible dans son milieu au moyen des similitudes qu'elle a avec une image étalon de la cible. Ce rapport présente une évaluation de la performance de l'algorithme séquentiel pour la détection de la similarité (ASDS) dans la détection numérique d'images. On montre que la performance de l'ASDS est comparable à celle de la méthode courante de corrélation mathématique. Les deux techniques sont décrites et essayées sur des photographies. Une évaluation analytique de l'ASDS appliquée à des images binaires est présentée. (NC)

CRDV R-4097/77 (NON CLASSIFIE)

Bureau – Recherche et Développement, Ministère de la Défense nationale, Canada.
CRDV, C.P. 880, Courcelette, Qué. G0A 1R0.

"Digital Area Correlation Tracking by Sequential Similarity Detection"
by C. Munteanu

La corrélation d'images est une méthode efficace de poursuivre une cible qui ne possède pas de traits saillants. Ceci implique la détection d'une cible dans son milieu au moyen des similitudes qu'elle a avec une image étalon de la cible. Ce rapport présente une évaluation de la performance de l'algorithme séquentiel pour la détection de la similarité (ASDS) dans la détection numérique d'images. On montre que la performance de l'ASDS est comparable à celle de la méthode courante de corrélation mathématique. Les deux techniques sont décrites et essayées sur des photographies. Une évaluation analytique de l'ASDS appliquée à des images binaires est présentée. (NC)

CRDV R-4097/77 (NON CLASSIFIE)

Bureau – Recherche et Développement, Ministère de la Défense nationale, Canada.
CRDV, C.P. 880, Courcelette, Qué. G0A 1R0.

"Digital Area Correlation Tracking by Sequential Similarity Detection"
by C. Munteanu

La corrélation d'images est une méthode efficace de poursuivre une cible qui ne possède pas de traits saillants. Ceci implique la détection d'une cible dans son milieu au moyen des similitudes qu'elle a avec une image étalon de la cible. Ce rapport présente une évaluation de la performance de l'algorithme séquentiel pour la détection de la similarité (ASDS) dans la détection numérique d'images. On montre que la performance de l'ASDS est comparable à celle de la méthode courante de corrélation mathématique. Les deux techniques sont décrites et essayées sur des photographies. Une évaluation analytique de l'ASDS appliquée à des images binaires est présentée. (NC)

DREV R-4097/77 (UNCLASSIFIED)

Research and Development Branch, Department of National Defence, Canada.
DREV, P.O. Box 880, Courcelette, Que. G0A 1R0.

"Digital Area Correlation Tracking by Sequential Similarity Detection"
by C. Munteanu

Area correlation tracking is an effective method of tracking targets that do not have salient characteristics. This involves detecting a target within a scene by means of its similarity with a stored image of the target. This report presents an evaluation of the performance of a sequential similarity detection algorithm (SSDA) in the task of digital image detection. It is shown that the performance of the SSDA is highly competitive with that of the widely used mathematical correlation method. Both techniques are reviewed and tested on still photographs. An analytical evaluation of the SSDA applied to binary images is presented. (U)